ORIGINAL ARTICLE

Non-linear station motions in epoch and multi-year reference frames

Mathis Bloßfeld · Manuela Seitz · Detlef Angermann

Abstract In the conventions of the International Earth Rotation and Reference Systems Service (e.g. IERS Conventions 2010), it is recommended that the instantaneous station position, which is fixed to the Earth's crust, is described by a regularized station position and conventional correction models. Current realizations of the International Terrestrial Reference Frame use a station position at a reference epoch and a constant velocity to describe the motion of the regularized station position in time. An advantage of this parameterization is the possibility to provide station coordinates of high accuracy over a long time span. Various publications have shown that residual non-linear station motions can reach a magnitude of a few centimeters due to not considered loading effects. Consistently estimated parameters like the Earth Orientation Parameters (EOP) may be affected if these non-linear station motions are neglected. In this paper, we investigate a new approach, which is based on a frequent (e.g. weekly) estimation of station positions and EOP from a combination of epoch normal equations of the space geodetic techniques Global Positioning System (GPS), Satellite Laser Ranging (SLR) and Very Long Baseline Interferometry (VLBI). The resulting time series of epoch reference frames are studied in detail and are compared with the conventional secular approach. It is shown that both approaches have specific advantages and disadvantages, which are discussed in the paper. A major advantage of the frequently estimated epoch reference frames is that the non-linear station motions are implicitly taken into account, which is a major limiting factor for the accuracy of the secular frames. Various test computations and comparisons between the epoch and secular approach are performed. The authors found that the consistently estimated EOP are systematically affected by the two different combination approaches. The differences between the epoch and secular frames reach magnitudes of 23.6 µas (0.73 mm) and 39.8 µas (1.23 mm) for the x-pole and y-pole, respectively, in case of the combined solutions. For the SLR-only solutions, significant differences with amplitudes of 77.3 µas (2.39 mm) can be found.

1 Introduction

The most recent realization of the International Terrestrial Reference System (ITRS) is the International Terrestrial Reference Frame 2008 (ITRF2008; Altamimi et al. 2011), which was computed at the Institut Géographique National (IGN) and is available at ftp://itrf.ign.fr/pub/itrf/. Another realization of the ITRS is the DGFI Terrestrial Reference Frame 2008 (DTRF2008), which was computed at the Deutsches Geodätisches Forschungsinstitut (DGFI) in Munich (Seitz et al. 2012) and is available at ftp://ftp.dgfi.badw.de/pub/DTRF2008. Both reference frames consist of coordinates and velocities of globally distributed stations of the space geodetic techniques Global Navigation Satellite System (GNSS), especially the Global Positioning System (GPS), Satellite Laser Ranging (SLR), Very Long Baseline Interferometry (VLBI) and Doppler Orbitography and Radiopositioning Integrated on Satellites (DORIS). Besides the station positions and velocities, both TRS realizations contain consistently estimated Earth Orientation Parameters

M. Bloßfeld (✉) · M. Seitz · D. Angermann
Deutsches Geodätisches Forschungsinstitut (DGFI),
Alfons-Goppel-Straße 11, 80539 Munich, Germany
e-mail: blossfeld@dgfi.badw.de

(Altamimi et al. 2011; Seitz et al. 2012), abbreviated with EOP in the following.

In the ITRF2008 and the DTRF2008, the motion of a station over time is conventionally realized as a position at a reference epoch and a constant velocity. Since the velocity can be used to compute a position at any epoch (also many years apart from the reference epoch), this kind of TRF is called a multi-year reference frame (MRF) hereafter. The advantage of this type of parameterization is that the station positions and velocities are derived with very high precision and that the reference frame shows a high long-term stability. This is fundamental for applications dealing with the monitoring of long-term changes within the Earth system, e.g. global sea level variations (Blewitt 2003; Seitz 2009).

In contrast to the advantages of the linear station motion, there are also some disadvantages using the common parameterization:

(i) Abrupt changes or non-linear movements like periodical motions or post-seismic behavior after an earthquake could falsify the computed station velocities dramatically (Blewitt and Lavallée 2002; Meisel et al. 2005; Angermann et al. 2007; Bloßfeld et al. 2012a).

(ii) The velocity of such a fragment can only be estimated stably, if enough observations spread over a period more than 2.5 years (Blewitt and Lavallée 2002; Angermann et al. 2007) are available. This means that stable station positions might not be computable for a period of about 2.5 years after an earthquake.

(iii) The approximation of the station motion with a linear velocity suppresses non-linear motions (e.g. van Dam et al. 1994, 2012; Petrov and Boy 2004; Tregoning and van Dam 2005; Collilieux et al. 2009; Tregoning and Watson 2009; Davis et al. 2012), which may be either absorbed by the observation residuals of the adjustment or propagate into consistently estimated or reduced parameters.

(iv) If the MRF is applied at a certain epoch t_i, the obtained station positions are regularized station positions and are not equal to the instantaneous station positions (Petit and Luzum 2010). The differences are caused by the not-parameterized non-linear station motions.

To overcome these problems, an epoch-wise (weekly) realization of the ITRS was performed by combining GPS, SLR and VLBI epoch normal equations. Compared to technique-individual weekly solutions, the combination allows to make use of the strengths of each space geodetic technique.

In the ERFs, station coordinates and EOP are adjusted. In contrast to the MRF solution, no station velocities are estimated. The reference frames computed epoch-wise are called epoch reference frames (ERFs) hereafter. For the first time, a long time series of ERFs is computed. Due to the fact that the

reference frame realizations are based on identical input data, differences in the EOP time series are solely caused by (i) the different station parameterization and (ii) the uncertainty of the realized datum and the limited and variable number of available local ties in the ERFs.

A major goal of this paper is to study this new approach in detail and to evaluate the advantages and disadvantages of the epoch reference frames w.r.t. the conventional secular approach, using long-term time series of data from multiple techniques. The structure and contents of the paper are summarized below. Section 2 deals with the basic theory of the station parameterization for the MRF and the ERF and the realization of the TRF datum (origin, orientation, scale). Therein, we examine the properties of the different observation techniques and TRF realizations. In Sect. 3, the data used and the parameter representation are described. Section 4 presents the methodology to compute ERFs and MRFs in detail. The computation strategies of each TRF realization are characterized and compared to each other. In Sect. 5, the technique-dependent and combined MRF and ERF realizations are validated w.r.t. the DTRF2008. The particular EOP time series are compared to the 08 C04 time series (ftp:// hpiers.obspm.fr/iers/eop/eopc04) of the International Earth Rotation and Reference Systems Service (IERS). In Sect. 6, the pros and cons of the ERF and the MRF are discussed. The effects of the non-linear station motions on the consistently adjusted EOP are studied in detail. Finally, the major findings and results are summarized.

2 Theoretical foundations

2.1 Parameterization of station movements

The instantaneous position of a station $X(t)$, which is fixed to the Earth crust, is defined in the IERS Conventions 2010 (Petit and Luzum 2010) as the sum of a regularized station position $X_R(t)$ and n conventional corrections $\sum_n \Delta X_n(t)$

$$X(t) = X_R(t) + \sum_n \Delta X_n(t). \qquad (1)$$

In the conventional secular approach, the regularized station position itself is parameterized by a linear model describing the position at any epoch t_i by the position at the reference epoch t_0 plus a constant velocity multiplied by the time difference $(t_i - t_0)$

$$X_R(t_i) = X_R(t_0) + \dot{X} \cdot (t_i - t_0). \qquad (2)$$

The non-linear station displacements could be divided into four categories:

(i) conventional displacements of reference markers on the crust, modeled with $\sum_n \Delta X_n$ (e.g. tidal motions),

(ii) non-conventional (non-modeled) displacements of reference markers (non-tidal motions),
(iii) modeled displacements of the technique-dependent internal reference points,
(iv) non-modeled displacements of the technique-dependent internal reference points.

The conventional displacements (i) are approximated by models considering the effects on stations due to solid Earth tides, ocean loading, rotational deformation due to polar motion and ocean pole tide loading (Petit and Luzum 2010). Even if these various effects are conventionally modeled, one has to keep in mind that model uncertainties, model inconsistencies and possible model errors could falsify the corrections of the instantaneous station position.

For the non-conventional (non-tidal) displacements (ii) due to, e.g. atmospheric or hydrological environmental loads, the IERS Conventions 2010 do not recommend any correction model at the moment (e.g. due to the fact that the current models are not accurate enough). Various investigations (e.g. van Dam et al. 1994, 2012; Petrov and Boy 2004; Tregoning and van Dam 2005; Collilieux et al. 2009; Tregoning and Watson 2009; Davis et al. 2012) have shown that periodic variations in the time series of station positions with amplitudes up to several centimeters are caused by neglected corrections such as surface loading. Bevis et al. (2005) found annual variations in the height component of the GPS station in Manaus with a peak-to-peak amplitude of 50 to 75 mm which are caused by the elastic response of the lithosphere to mass changes of a flowing river system. To ensure consistency with these conventions, the space geodetic data used for this investigation are not corrected for atmospheric and hydrological loading effects. Another important issue is the post-seismic behavior of a station which can last over decades and is non-linear in time (Bürgmann and Dresen 2008; Freymueller 2010). For example, Suito and Freymueller (2009) found surface motions of 15–20 mm/year w.r.t. long-term movements even 45 years after the 1964 Alaska earthquake. Besides the geophysical effects, also anthropogenic periodic effects like, e.g. yearly groundwater withdrawal (Bawden et al. 2001) differ from a linear signal.

Models for the displacement of internal reference points (iii) are mostly technique-dependent and are provided (updated) by the particular technique services of the International Association of Geodesy (IAG) if necessary. The International VLBI Service (IVS), for example, recommends to correct the observations for the effect of thermal deformation of the radio antenna (Nothnagel 2009).

The fourth category (iv) contains all non-modeled technique-dependent displacements of internal reference points (e.g. gravitational deformation of the radio antenna Sarti et al. 2011), which need to be further studied.
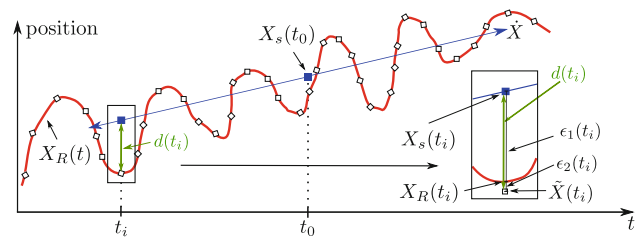

Fig. 1 Station motion parameterization of a multi-year (*blue*, continuous linear) and an epoch reference frame (*white boxes*, discrete). The regularized station position (*red*, continuous non-linear) can be approximated more accurately with an estimation of weekly station positions than by an extrapolation with a constant velocity in time

Since the applied correction models are not totally perfect and some effects are still not modeled or cannot be modeled accurately, the motion of the regularized station position $X_R(t)$ is not linear. To take these systematics into account, an alternative parameterization of this station motion is investigated in this study. In contrast to a secular MRF represented by $X_s(t_0)$ and $\dot{X}$, time series of epoch reference frames (ERFs) with a weekly resolution are estimated. A weekly time interval was chosen, because the SLR standard solution is weekly arcs. In future investigations, it might be worthwhile to investigate also other resolutions. These ERFs contain station positions at epochs t_i with a step size $h = t_{i+1} - t_i$ of one week. A certain position $\tilde{X}(t_i)$ is assumed to be constant only within the respective time interval $[t_i - h/2; t_i + h/2]$. Figure 1 emphasizes that the ERF allows a much better approximation of the regularized station position $X_R(t_i)$ than the MRF does.

From Fig. 1, we find that

$$X_s(t_i) + \epsilon_1(t_i) = X_R(t_i) = \tilde{X}(t_i) + \epsilon_2(t_i) \tag{3}$$

with $\epsilon_1(t_i)$, $\epsilon_2(t_i)$ being the approximation errors of the different parameterization and $\epsilon_1(t_i) \gg \epsilon_2(t_i)$. As shown in Fig. 1, the linear station motions are considered in both frame types. The non-linear differences $d(t_i) = \epsilon_2(t_i) - \epsilon_1(t_i)$ between the conventional parameterization and the positions estimated epoch-wise are dominated by seasonal effects and can reach amplitudes up to several centimeters (van Dam et al. 1994, 2012; Petrov and Boy 2004; Bevis et al. 2005; Tregoning and Watson 2009; Bloßfeld et al. 2012b; Davis et al. 2012) although they are commonly much smaller.

The non-linear differences can be split up into four parts:

- $d^i(t)$: individual non-linear station motion caused by, e.g. local environmental effects (e.g. Bawden et al. 2001).
- $d_t^c(t)$: non-linear station motions common to all stations which cause variations in the barycenter of the network (only common translations).
- $d_r^c(t)$: non-linear station motions common to all stations which cause variations in the orientation of the network (only common rotations).

– $d_s^c(t) = (0, 0, \Delta h(t))$: non-linear station motions in the height component common to all stations which only cause variations in the scale.

Collilieux et al. (2009, 2012) showed that loading signals partly alias into $d_t^c(t)$, $d_r^c(t)$ and $d_s^c(t)$. This means that the non-modeled loading signals cause variations in the barycenter, the orientation and the scale of a station network. The non-linear motion (in north, east and height), which is intrinsic to a station, can be computed with

$$d^i(t_i) = d(t_i) - [d_t^c(t_i) + d_r^c(t_i) + d_s^c(t_i)]. \tag{4}$$

The common station motions are discussed in the following three sections and in Sect. 5, the individual station motions are discussed in Sect. 6.1.

2.2 Origin of terrestrial reference frames

The origin of a terrestrial reference frame can be defined amongst others, as

– Center of Mass (CM) of the whole Earth (solid Earth plus its fluid envelope; Blewitt 2003; Dong et al. 2003; Tregoning and van Dam 2005; Wu et al. 2012). The CM is here defined to be invariant ($CM \equiv 0$).
– Center of Figure (CF). In the literature, various definitions of the Figure of the Earth exist. Listing (1873) designated the geoid as the surface of constant gravity potential. This definition can be seen as the mathematical figure of the Earth (Torge 2001). If an infinite number of stations homogeneously distributed on the geoid would be available (including the geoid over the oceans!), the CF would be the barycenter of such an ideal network.

Since we are dealing with a finite number of observing stations spread inhomogeneously on the Earth's crust (only on the continents and some islands), we have to introduce two other definitions:

– Origin of Network (ON). The $ON(t)$ is the origin of the coordinate system which is realized through the station coordinates at the epoch t.
– Center of Network (CN). The $CN(t)$ is the barycenter of a station network at the epoch t (Dong et al. 2003; Tregoning and van Dam 2005; Wu et al. 2012).

Through the satellite orbit dynamics, SLR observations are sensitive to the CM. This means that for an SLR-only and a combined TRF, its $ON(t)$ coincides with the CM at every observation epoch. In principle, the same holds for GPS (and DORIS), but due to technique-specific model uncertainties, a singularity w.r.t. the origin is artificially created by introducing translation parameters referred to all stations in the NEQ. Therefore, the $ON(t)$ of the GPS-only (and the DORIS-only)

TRF is neither accessible any longer nor equal to the CM (see also Blewitt 2003; Dong et al. 2003). The same holds for VLBI data since the observations do not provide information to realize the origin of the network. According to Dong et al. (2003), the realization of the CF is very difficult or even impossible. In reality, the barycenter of the station network strongly depends on the global station distribution. Thus, it varies over time and between different geodetic space techniques. The barycenter $CN(t)$ for a network of N stations is computed with

$$CN(t) = \frac{1}{N} \sum_{k=1}^{N} X_k(t). \tag{5}$$

In the case of GPS and VLBI, the rank deficiency has to be removed by applying a No-Net-Translation (NNT) condition (Angermann et al. 2004; Seitz 2009) w.r.t. the a priori coordinates. The NNT condition ensures that the $CN(t)$ of the adjusted TRF is equal to the $CN(t)$ of the a priori TRF (see Table 1). It is important to note at this point that not all stations are used for the NNT condition. A homogeneously distributed station network is selected based on different criteria such as stable and long coordinate time series of the stations. The selection is to a certain extent subjective. If such a global evenly spread network can be chosen, the difference between the $CN(t)$ of the subnetwork and the CF can be reduced (but an offset would remain!). Nevertheless, due to the selection of a subnetwork, the $CN(t)$ of the whole network is still not equal to the $CN(t)$ of the whole a priori network. For a TRF with a linear station motion model, the offset between the CF and the $CN(t)$ is not constant. Since the kinematic models do not include all motions viewed from the CF, the $CN(t)$ drifts w.r.t. the CF (Dong et al. 2003). The same holds for the SLR-only and the combined ERF. Additionally, their $CN(t)$ show a non-linear variation w.r.t. the $CN(t)$ of the corresponding MRF. The differences are partly caused by the different station parameterization $d_t^c(t)$ of the ERF and the MRF (see Sect. 2.1 and Collilieux et al. 2009).

Table 1 summarizes the characteristics of the different space techniques w.r.t. the definitions given above.

2.3 Orientation of terrestrial reference frames

The orientation of the ITRS is defined to be the orientation initially given by the BIH (Bureau International de l'Heure) at 1984.0. Its time evolution should be aligned to horizontal tectonic motions over the whole Earth (Petit and Luzum 2010). A conventional way to realize the orientation of a TRF is to apply a geocentric No-Net-Rotation (NNR) condition (Angermann et al. 2004; Seitz 2009) w.r.t. an a priori TRF. This means that no common rotations $d_r^c(t)$ of the adjusted TRF w.r.t. the a priori TRF are allowed. As it was the case

Table 1 Position and motion of $ON(t)$ and $CN(t)$ w.r.t. CM over time

Tech.	Type	$ON(t)$	$CN(t)$
GPS	MRF	n.a.	Offset, drift
	ERF	n.a.	$CN_{MRF}(t)$
VLBI	MRF	n.a.	Offset, drift
	ERF	n.a.	$CN_{MRF}(t)$
SLR	MRF	CM	Offset, drift (o.d.)
	ERF	CM	o.d., non-linear variation $d_t^c(t)$
Comb.	MRF	CM	Offset, drift (o.d.)
	ERF	CM	o.d., non-linear variation $d_t^c(t)$

(n.a.) means that this quantity is not accessible since for GPS, translation parameters are introduced in the NEQ and VLBI is not sensitive to the CM at all. $CN_{MRF}(t)$ means the $CN(t)$ of the MRF

for the NNT condition, the NNR condition is applied only for a subnetwork of stations. This means that the adjusted TRF shows no rotation w.r.t. the a priori TRF. Additionally, the translation of a network has to be taken into account when applying a geocentric NNR condition. Kreemer et. al (2006) showed that a significant translation of a TRF (change in $CN(t)$) has an impact on the NNR condition and, therefore, on the TRF orientation. Also Collilieux et al. (2012) mentioned that the rotation parameters used to constrain a frame orientation (NNR condition) are biased by loading effects.

Within the MRFs, normally an adequate network for the NNR condition can be chosen. In the case of the ERFs, especially the sparse networks in the VLBI-only and SLR-only TRFs are critical for the datum realization. For the GPS-only and the VLBI-only ERF, the translations of the $CN(t)$ of the subnetwork w.r.t. the $CN(t)$ of the a priori subnetwork are set to zero via the NNT condition. Consequently, the geocentric NNR condition is not biased if the same subnetwork as for the NNT condition is used.

The situation for the ERFs which contain SLR data is different. Since no NNT condition is applied and the observation network within, e.g. 1 week is sparse, the NNR condition is biased by a weekly translation $d_t^c(t)$ of the selected subnetwork.

The EOP are complementary parameters to the network orientation and describe geocentric (around CM) global rotations of all stations of a TRF. If the NNR condition is applied only on a subnet of stations, the remaining common rotations of the non-datum stations will affect the EOP. Since the NNR condition is applied only once (at the reference epoch) on an MRF, only the offset and the drift of the consistently estimated EOP are affected. In the case of the ERF (which include SLR data), the biased NNR condition is applied at every epoch t. Consequently, also the EOP are affected at every epoch t. This is a clear disadvantage of the SLR-only ERF which could only be eliminated if the weekly observation network is more homogeneous and/or by an improved modeling of the non-linear station motions.

2.4 Scale of terrestrial reference frames

According to Petit and Luzum (2010), the unit length of the ITRF is the meter (SI). The ITRF scale is realized as a mean scale of SLR and VLBI. For GPS, Schmid et al. (2007), Ray et al. (2008), Collilieux et al. (2012) stated that technique specific effects like phase center offsets bias the GPS-only TRF scale. To overcome this problem, a rank deficiency w.r.t. the scale is artificially created (introduction of a scale parameter). To realize the network scale, a No-Net-Scale (NNS) condition is applied on a subnetwork of GPS stations (Angermann et al. 2004). The NNS condition ensures that there is no scale difference between the adjusted TRF and the a priori TRF. As for the NNR condition, the translations have to be taken into account when applying a NNS condition. Collilieux et al. (2012) found that there is also an effect of the weekly translations $CN(t)$ on the scale parameter as it was the case for the rotations (previous section).

3 Input data

The GPS solution was computed at the Technische Universität München (TUM), Institut für Astronomische und Physikalische Geodäsie (IAPG). From the daily SINEX (Solution Independent Exchange Format) files, constraint-free GPS-only NEQs (normal equations) are reconstructed (Seitz 2009). The SLR-only NEQs were computed at DGFI with DOGS-OC (Gerstl 1997), a library for Orbit Computation of the DOGS software package (DGFI Orbit and Geodetic parameter estimation Software). A manual of the entire software package (in German) is available at the website of the DGFI SLR analysis center (http://www.ilrs.dgfi.badw.de). The VLBI input is a combination of two individual VLBI-only NEQs which were computed at the Universität Bonn, Institut für Geodäsie und Geoinformation (IGG) and at DGFI. The combination of the individual VLBI-only NEQs to one combined NEQ per session was done at IGG. The data cover the time span from 1994.0 to 2007.0 (Table 2).

Table 2 Input data for the reference frame computation

Tech.	Solution type	Time span	Temporal resolution	References
GPS	Constrained solution	1994.0–2007.0	daily (0 h to 0 h)	Rothacher et al. (2011)
VLBI	Constraint-free NEQ	1994.0–2007.0	Daily (session-wise)	Rothacher et al. (2011)
SLR	Constraint-free NEQ	1994.0–2007.0	Weekly	This paper

Table 3 Parameters and their representation in the different technique-specific NEQs

Parameter	Tech.	Parameterization
Station coordinates [m]	GPS	Daily position
	VLBI	Daily position
	SLR	Weekly position
Terrestrial pole coordinates [mas]	GPS	pwl[a] with offsets at 0 h
	VLBI	Offset/drift at mid-epoch
	SLR	pwl[a] with offsets at 0 h
ΔUT1 = UT1−UTC [ms]	GPS	pwl[a] with offsets at 0 h
	VLBI	Offset/drift at mid-epoch
	SLR	pwl[a] with offsets at 0 h
Celestial pole coordinates [mas]	GPS	pwl[a] with offsets at 0 h
	VLBI	Offset/drift at mid-epoch
Gravity field coefficients (d/o 2)	SLR	weekly offset

[a] A piece-wise linear polygon representation

For the analysis of the observations of all three techniques, the homogenized models of the GGOS-D project (Table 2; Rothacher et al. 2011) were used. The use of identical and consistent models within the analysis of intra- and inter-technique combinations is essential to avoid systematic differences in the solutions which could lead to misinterpretations. As an example, Böckmann et al. (2007) found VLBI station height differences up to 15 mm due to different pole tide models. Table 3 gives an overview of the parameters and their representation as they are included in each NEQ. Satellite- and technique-dependent parameters as well as tropospheric parameters are pre-reduced. As it is shown in Angermann et al. (2004), Thaller (2008), Seitz (2009), Seitz et al. (2012), it has to be ensured that NEQs with the same length of the parameter vector and the same parameter representation (parameterization and a priori values) are combined. In case of the VLBI EOP, the transformation of the offset and drift representation at the mid-epoch of each session into the piece-wise linear representation at the midnight epochs of the terrestrial and the celestial pole coordinates is done according to Thaller (2008), Seitz (2009). In the case of UT1 (Universal Time) and LOD (Length Of Day), the interpolation is divided into three steps:

(i) reduction of [ΔUT1, LOD] to [ΔUT1$_R$, LOD$_R$] by tidal signal corrections according to the IERS Conventions 2010 (ΔUT1 = UT1−UTC)

(ii) parameter transformation with [ΔUT1$_R$, LOD$_R$] to offsets at 0 h epochs (like the terrestrial pole coordinates)

(iii) conversion of ΔUT1$_R$ offsets at 0 h epochs to ΔUT1 offsets at 0 h (re-adding the respective tidal signal corrections at the 0 h epochs)

4 Computation algorithm

The computation of global terrestrial reference frames at DGFI is based on the combination at the normal equation level (Angermann et al. 2004, 2007; Meisel et al. 2005; Seitz 2009; Bloßfeld et al. 2012b; Seitz et al. 2012) with DGFI's combination software called DOGS-CS (Gerstl et al. 2001), the library for Combination and Solution of DOGS. As input data for the multi-year reference frame and the time series of epoch reference frames, identical NEQs as described in Sect. 3 are used. The differences of the gravity field coefficients between the MRF and the ERF solution are not considered in this paper. To avoid any inconsistencies between the ERF and the MRF solution, the coefficients are fixed to the same gravity field solution EIGEN-GL04C1 (Förste et al. 2008).

4.1 Multi-year reference frames (MRFs)

The computation algorithm for DGFI's MRFs comprises two steps: the intra-technique and the inter-technique combination (Fig. 2, right chain).

Before combining the different techniques, the time series of station positions have to be analyzed with regard to dis-
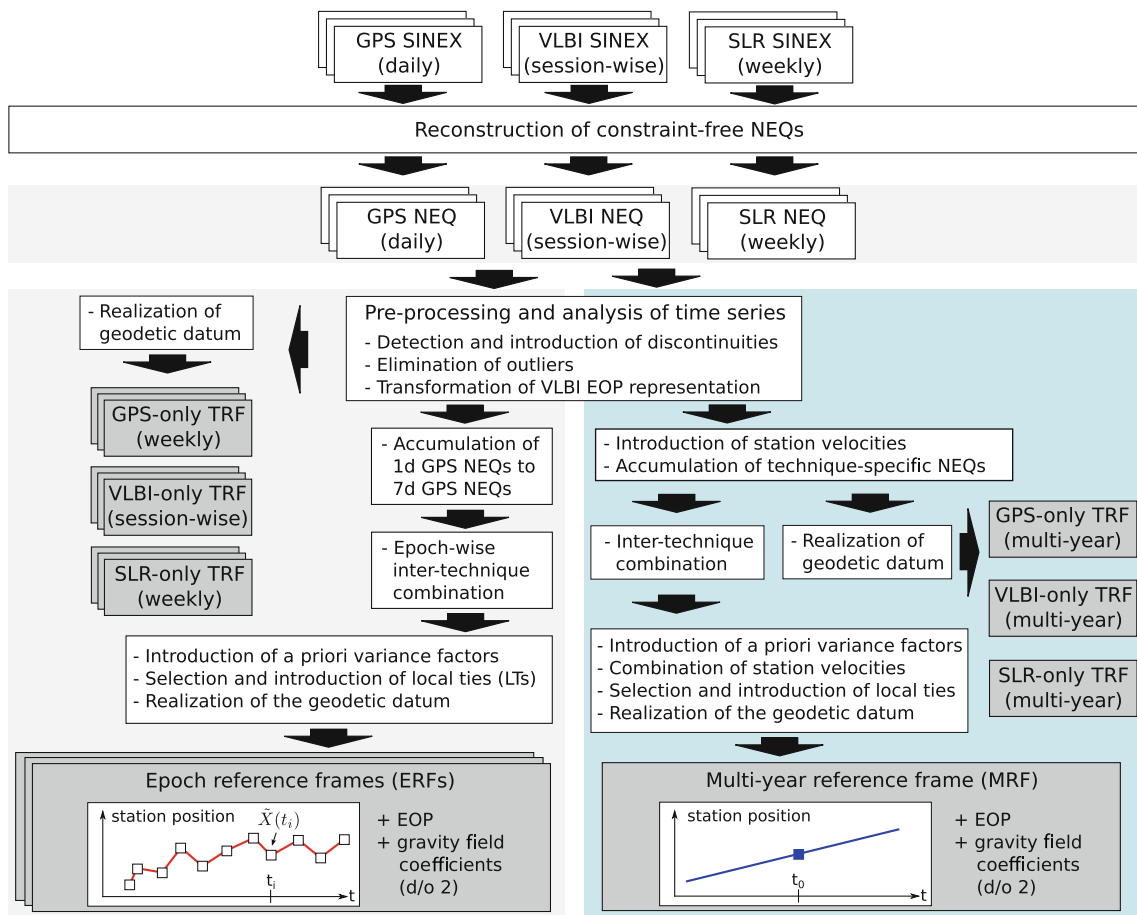
Fig. 2 Processing scheme for epoch and multi-year reference frames. Both reference frame types are based on identical input data. In total, four different solution types are computed: technique-specific ERFs, combined ERFs, technique-specific MRFs and a combined MRF

continuities, post-seismic behavior after earthquakes, outliers and other non-linear effects. Therefore, epoch-wise technique-specific solutions are computed. If any outliers in a station position, time series are detected, they have to be removed before the combination process is continued. Otherwise, they would falsify the estimated station position and velocity within the multi-year solution. An epoch coordinate is defined as an outlier if the absolute value in one component (x, y, z) of the adjusted correction is three times larger than its standard deviation. Abrupt changes or non-linear post-seismic motions are approximated by piece-wise linear station positions. For each station, constant velocities are set up as new parameters in the equation system.

Afterwards, the NEQs are accumulated. Common parameters such as station coordinates, velocities and EOP at the week boundaries are stacked. The stacking of the coordinates is done for all available stations in the epoch NEQs. Therefore, the non-linear motions of every station in the MRF NEQ are neglected and the $CN(t)$ can vary only linearly in time. The suppressed non-linear $CN(t)$ variation, if not absorbed

by artificially created singularities (Sect. 2.2), is forced into the observation residuals or other parameters. Approaches that consider the non-linear $CN(t)$ variation in the accumulation process are critical. If translation parameters are introduced in every epoch NEQ and the origin is realized after the accumulation through an NNT condition, the origin of the network is not equal to the CM any longer. In an ideal case, with an infinite number of station used for the NNT condition, the CF can be realized.

Besides the translations, also the scale is affected by the neglected loading signals (see Sect. 2.4). Due to the fact that the loading signals have mainly a seasonal character (Sect. 2.1), the effects on the translations and the scale are expected to be dominated by a seasonal variation. In the case of the GPS-only NEQs, prior introduced rank deficiencies w.r.t. the origin and the scale absorb this variation. Within the VLBI-only NEQs, there is no sensitivity w.r.t. the CM at all; therefore, the non-linear $CN(t)$ variation is absorbed by the not accessible origin.

Solely the SLR-only NEQs are sensitive to the CM. Since the non-linear translations cannot propagate into the linear

moving $CN(t)$ or the scale, they are forced partly via the correlation of translations and rotations into the orientation of the network.

Within all NEQs, the orientation is a singularity (degree of freedom, Sect. 2.3). Thus, due to the inhomogeneous station distribution and the resulting correlation between the translation and the rotation of the station network, the not-considered epoch-wise $CN(t)$ variation affects the orientation of the NEQs. For an SLR-only NEQ, the correlation is higher than for a GPS-only NEQ, since the GPS station network is distributed more homogeneously. Finally, due to the one-to-one relation of the network orientation and the EOP, also the EOP (being epoch parameters) are affected by the $CN(t)$ variation and reflect the orientation differences very well.

The result of the intra-technique combination process is one NEQ per technique with station positions, velocities and EOP. At the end of this first processing step, the obtained NEQs are used to compute single-technique MRFs. Therefore, the technique-specific NEQs are solved. Due to the rank deficiencies of the NEQs, the datum has to be realized with additional conditions. For GPS, an NNT, an NNR and an NNS condition w.r.t. a selected subnetwork are applied to the NEQ. For SLR, only an NNR condition is applied whereas for VLBI, an NNT and an NNR condition are added to the NEQ.

Within the inter-technique combination, the individual NEQs are equally weighted (based on the a posteriori variance factor of each single-technique NEQ). The EOP as the only parameters common to all techniques are stacked. The coordinates of stations at co-location sites (sites with two or more techniques available) are different parameters and could not be stacked directly. To link the station positions, terrestrial measured difference vectors (local ties) between the individual reference points are introduced as pseudo observations. The selection of the local ties (LTs) and the determination of the relative weight of these condition equations w.r.t. the NEQ are a complex process. According to Seitz et al. (2012), the selection is done by comparing the LTs with the 3D-difference vector of the single technique solutions. Seitz et al. (2012) investigated various combinations of different thresholds for the 3D-difference and standard deviations for the pseudo observations. They validated the variables w.r.t. to the network deformation and the effect on the terrestrial pole coordinates. With a threshold between 28 and 36 mm and a standard deviation of 0.5 to 1.0 mm, they obtained the best results. For this study, a set of currently available LTs from the DGFI ITRS Combination Center is used. The LTs are selected with a threshold of 30 mm and $\sigma = 1.0$ mm. The station velocities of co-located instruments are combined if the absolute value of the difference of the single-technique MRF velocities is smaller than 1.5 mm/a and if the velocity difference is accepted by the 3σ-criteria. The combination is done using pseudo observations of the form ($v_1 - v_2 = 0$) with a standard deviation $\sigma = 0.1$ mm/a.

The origin of the NEQ is the CM which is realized by SLR (see Table 1). The scale is realized as an SLR and VLBI mean scale. As was the case for the SLR-only MRF, the orientation and therewith the EOP of the combined NEQ are affected by the neglected $CN(t)$ variation. To remove the remaining rank deficiency w.r.t. the orientation of the combined NEQ, a NNR condition w.r.t. the DTRF2008 using a subset of stable GPS stations (long continuous time series, low scatter of the position time series and homogeneous global distribution) has to be applied. The fact that only the orientation has to be realized with an additional condition is one advantage of the combination of different geodetic space techniques. Nevertheless, the NNR condition is biased through a translation offset and rate of the MRF (see Sect. 2.3).

One has to keep in mind that applying the combined MRF at an epoch t means getting regularized positions $X_s(t)$ in a CM frame.

4.2 Epoch reference frames (ERFs)

As a supplement to multi-year reference frames, time series of epoch reference frames are computed (left chain in Fig. 2). In contrast to the MRF, no station velocities have to be introduced as new parameters in the NEQs, because the station motion is approximated implicitly by the coordinate time series. Abrupt changes in the station coordinates are considered directly by the epoch reference frame time series, since the station coordinates are assumed to be constant only for the specified time interval (see Sect. 2.1). If an abrupt change happens within the time interval, the station is removed for that interval. For this study, an interval of one week is chosen because the arc length of the SLR solutions is seven days. The outliers detected within the MRF computation are also used for the ERF computation. One has to keep in mind that in one single ERF-NEQ, there are much less observations contributing to the solution than in the accumulated NEQ of a multi-year solution. Therefore, the impact of a remaining outlier on the solution is much higher. The higher sensitivity of the realized datum on the estimated parameters is visible in the epoch datum parameters which are shown in Sect. 5. If the number of stations in the ERF would be less than three, it can be necessary to keep an identified outlier in the ERF NEQ although it is removed in the MRF NEQ. The same holds for the situation when less than three co-located stations on different continents are included in the combined NEQ. After the detected outliers are removed, the parameterization of the different technique-specific NEQs has to be homogenized. In particular, the VLBI EOP have to be transformed from an offset and drift representation at the mid-epoch of the session to two offsets at the day boundaries (Sect. 3).

Each time series of single-technique NEQs is used to compute a time series of technique-specific ERFs. The single-technique NEQs have the same rank deficiencies as was described for the single-technique MRFs in Sect. 4.1 (except of the velocity part). To remove the rank deficiencies, additional conditions were added to each epoch NEQ in the time series.

The origin of the SLR-only ERFs always coincides with the CM. Within 1 week, the real station position is approximated with a constant position. Subweekly variations, which are not modeled, are forced into the observation residuals or may affect other epoch parameters such as the daily EOP. The Center of Network $CN(t)$ of the SLR-only ERF shows, in contrast to the MRF, the variations in time caused by the loading signals since it is not forced to move linearly. Therefore, the non-linear $CN(t)$ variation does not alias into other parameters as it is the case for the SLR-only MRF.

For the epoch combinations, seven successive daily GPS NEQs are accumulated to form one weekly GPS NEQ. VLBI is not providing successive NEQs, except for the Continuous VLBI campaign periods (CONT campaigns; http://www.ivscc.gsfc.nasa.gov). Therefore, the VLBI session NEQs are combined with the weekly GPS/SLR NEQ individually.

The relative weights of the different NEQs are computed according to Seitz (2009). The method described there is based on the variation of the station position time series. The main idea is that the mean standard deviations of the station positions of two observation techniques should have the same ratio as the mean standard deviations derived from the technique-specific station position time series. The relative weights for each epoch combination are 0.12 for the GPS-only NEQ and 1.00 for the SLR-only and the VLBI-only NEQ. The GPS-only NEQ has to be down-weighted because neglected correlations between the GPS observations result in too optimistic standard deviations of the parameters included in the GPS-only NEQ (Schön and Kutterer 2007). The obtained weights depend strongly on the selection of the stations used for the computation of the mean standard deviation. To get realistic weights, only stations with a stable coordinate time series are used. It is assumed that the weights are constant over time.

For the computation of epoch reference frames, the selection and the relative weight of the LTs is a critical issue since the epoch NEQs are much more sensitive on these quantities. This is why we choose (according to Seitz et al. 2012 and Sect. 4.1) a standard deviation of 1.0 mm for the LTs. For the ERFs, the number of stations per week is increasing since 1994.0 (Fig. 4). To get stable results during the first years and to ensure that almost the same amount of LTs is available during the whole time span, the selected threshold for the epochs $t_i < 2,000.0$ is 50 mm and for the epochs $t_i \geq 2,000.0$, it is 30 mm (see Fig. 5). The chosen thresh-

olds ensure that about 80 % of the available LTs could be used.

After combining the individual NEQs, the geodetic datum has to be realized. The rank deficiency for the combined ERF NEQ is the same as for the combined MRF NEQ (except of the velocity part). The origin (CM) is realized through the SLR-only NEQ, the scale is equal to the SLR and VLBI mean scale and the orientation is realized by applying an NNR condition w.r.t. a subset of stable GPS stations.

Finally, the combined NEQs are solved and a long time series of inter-technique epoch solutions (GPS, SLR and VLBI) is computed. In contrast to an MRF, the ERFs provide regularized positions $\tilde{X}(t)$ in a CM frame at every epoch t where an ERF is available.

5 External validation of the solutions

5.1 Multi-year reference frames (MRFs)

In total, four multi-year reference frames are computed (GPS-only, SLR-only, VLBI-only and combined MRF). Each MRF contains a time series of NEQs (daily, weekly, session-wise) from 1994.0 to 2007.0 (Table 2). The computation was done as described in Sect. 4.1. To validate the quality of the MRFs, the obtained station coordinates are compared with station coordinates of the DTRF2008 (Seitz et al. 2012). The consistently estimated EOP are compared to the IERS 08 C04 time series.

5.1.1 Station coordinates

The station network of each individual MRF is transformed with a 14 parameter similarity transformation to the DTRF2008. For each transformation, the same subnet of stations as it is used for the datum realization is chosen. The transformation parameters and the corresponding rates are shown in Table 4. In the case of the single technique solutions, the origin and the orientation are realized with a maximum difference of -3.4 mm (at the Earth's surface) in the y-rotation of the SLR-only solution. The highest difference for the scale is obtained for the VLBI-only solution (1.5 mm).

In the case of the combined solution, the highest difference for the translation and rotation parameters is obtained for the SLR sub-network (4.5 mm in the z-rotation) whereas for the scale, a maximum offset of 4.3 mm w.r.t. the DTRF2008 is estimated for the GPS sub-network.

In the last column of Table 4, the root mean square (RMS) of the similarity transformation is shown. By comparing the RMS values of the single-technique solutions w.r.t. the combined solution, the positive effect of the combination can be seen (smaller RMS values for the SLR and VLBI sub-network of the combined solution w.r.t. the single-

Table 4 Transformation parameters obtained from the 14 parameter similarity transformation of the computed MRFs (single-technique solutions (upper part), technique-specific networks of the combined solution (lower part)) to the DTRF2008 at epoch 2,000.0

Tech.	Par. [mm] rate [mm/a]	t_x	t_y	t_z	r_x	r_y	r_z	Sc	RMS
GPS	Parameter	0.0 ± 0.2	0.9 ± 0.2	-0.1 ± 0.2	0.1 ± 0.2	0.0 ± 0.2	0.5 ± 0.2	-0.2 ± 0.2	1.2
	Rate	-0.2 ± 0.2	0.3 ± 0.2	-0.2 ± 0.2	0.3 ± 0.2	0.0 ± 0.2	-0.1 ± 0.2	0.6 ± 0.2	
SLR	Parameter	0.1 ± 1.1	-1.2 ± 1.0	-0.7 ± 1.1	-0.1 ± 1.1	-3.4 ± 1.0	0.4 ± 1.1	-0.3 ± 0.9	3.3
	Rate	0.0 ± 1.1	-0.1 ± 1.0	-0.1 ± 1.1	-0.1 ± 1.1	-0.1 ± 1.0	0.1 ± 1.1	-0.1 ± 0.9	
VLBI	Parameter	0.3 ± 0.4	0.5 ± 0.4	-1.2 ± 0.4	0.7 ± 0.5	-1.0 ± 0.5	-0.9 ± 0.4	1.5 ± 0.4	1.9
	Rate	0.0 ± 0.4	0.5 ± 0.4	0.8 ± 0.4	0.4 ± 0.5	0.3 ± 0.5	-0.1 ± 0.4	0.1 ± 0.4	
Comb.	Parameter	1.1 ± 0.2	0.6 ± 0.2	0.5 ± 0.2	0.0 ± 0.2	-0.4 ± 0.2	0.6 ± 0.2	4.3 ± 0.2	1.2
(GPS)	Rate	0.0 ± 0.2	0.7 ± 0.2	-0.1 ± 0.2	0.3 ± 0.2	-0.1 ± 0.2	-0.1 ± 0.2	1.3 ± 0.2	
Comb.	Parameter	0.2 ± 0.9	-1.9 ± 0.8	-0.2 ± 0.9	3.0 ± 1.1	-3.9 ± 1.1	4.5 ± 1.1	0.0 ± 0.9	2.7
(SLR)	Rate	-0.1 ± 0.9	0.3 ± 0.8	0.0 ± 0.9	0.4 ± 1.1	-0.2 ± 1.1	0.5 ± 1.1	0.0 ± 0.9	
Comb.	Parameter	-0.7 ± 0.4	2.1 ± 0.4	1.8 ± 0.4	1.6 ± 0.5	0.0 ± 0.5	-1.3 ± 0.5	1.0 ± 0.4	1.5
(VLBI)	Rate	-0.2 ± 0.4	0.4 ± 0.4	0.7 ± 0.4	0.7 ± 0.5	0.0 ± 0.5	0.2 ± 0.5	0.2 ± 0.4	

Within the transformation, three translations (t_x, t_y, t_z), three rotations (r_x, r_y, r_z), a scale parameter (Sc) and the respective rates are estimated. The Root Mean Square (RMS) values of the transformations are given in the last column. The rotations and the scale are converted to displacements at the Earth's surface with the mean Earth radius $r_E = 6,378,137.0$ m

technique solutions). The small RMS values and the small estimated transformation parameters of the single-technique solutions as well as of the combined solution show that all MRFs agree well with one of the most recent realizations of the ITRS.

5.1.2 Earth orientation parameters

The EOP derived from the MRF solutions are compared to the IERS 08 C04 time series. The terrestrial pole coordinates of this time series are aligned to the ITRF2008 while the MRFs, discussed in this paper, are aligned to the DTRF2008 (via the NNR condition). Between the two ITRS realizations, there are small differences in the orientation (Table 18; Seitz et al. 2012): the x-rotations are below 0.5 mm for all technique-specific networks, the y-rotations are smaller than -1.3 mm.

Since the *x*- and *y*-orientation of the rotation axis of the station network and the terrestrial pole coordinates (y, x) are complementary parameters, small differences with the same order of magnitude of the terrestrial pole coordinates w.r.t. the IERS 08 C04 time series are expected. Figure 3 emphasizes the relationship between the different parameters and solutions w.r.t. the orientation. The weighted mean offsets between the Earth rotation parameters (x, y, ΔUT1) of the MRFs and the IERS 08 C04 time series are summarized in Table 5. The differences which are shown there can be explained by two different effects. The difference between the single-technique solutions and the combined solution results from the effect of the combination of the techniques. A part of the differences between all solutions and the IERS 08 C04 time series can be explained by the different datum
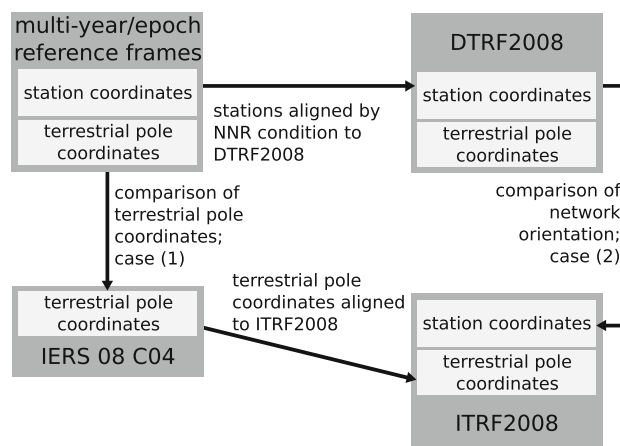
Fig. 3 Scheme of the relationship of the different solutions w.r.t. their orientations. The *x*- and *y*-orientation of the rotation axis of the station network and the terrestrial pole coordinates (y, x) are complementary parameters. The offsets between the terrestrial pole coordinates of the computed MRFs and the IERS 08 C04 time series (1) should be of the same order of magnitude as the orientation offsets between the ITRF2008 and the DTRF2008 (2)

realization of the solutions and the datum uncertainty of the ITRF2008, the DTRF2008 and the MRF solutions. In the following, *x*-pole denotes the *x*-coordinates of the terrestrial pole and *y*-pole denotes the *y*-coordinates, respectively.

The pole coordinate offsets of the GPS-only and the combined solution have the smallest standard deviations since the station networks are larger and distributed more homogeneous than the networks of the SLR- and VLBI-only solutions. Additionally, the larger number of observations in the case of GPS lead to a higher accuracy of the estimated para-

Table 5 Mean offsets and standard deviations of the terrestrial pole coordinates (x, y) and ($\Delta UT1$) of the single-technique and the combined multi-year solution w.r.t. the IERS 08 C04 time series

Technique	x-pole [µas]	y-pole [µas]	Δ UT1 [µs]
GPS	-52.0 ± 2.8	34.6 ± 2.4	–
SLR	-19.8 ± 8.7	-23.4 ± 8.3	–
VLBI	-77.8 ± 7.2	-0.2 ± 6.4	-4.5 ± 0.5
Combination	-72.4 ± 3.1	17.6 ± 2.6	1.1 ± 0.7

Fig. 4 Number of stations per week in the epoch reference frame time series. The sum of GPS stations (*green*), SLR stations (*blue*) and VLBI stations (*red*) is the total amount of stations (*black*) per week

Fig. 5 Number of local ties per week in the epoch reference frame time series: LTs between GPS and VLBI stations (*blue*), LTs between the GPS and SLR stations (*green*) and LTs between the SLR and VLBI stations (*red*). For VLBI, only LTs of different stations during one week are shown

meters. The standard deviations of the combined solution are larger than the standard deviations of the GPS-only solution, because the GPS-only NEQ is down-weighted in the combination. The pole coordinate offsets of the combined solution w.r.t. the IERS 08 C04 time series are -72.4 µas (-2.2 mm) for the x-pole and 17.6 µas (0.5 mm) for the y-pole (case (1) in Fig. 3). These differences agree well with the sum of two different effects: the differences in the realization of the MRF orientation (Table 4) and the differences between the orientation of the DTRF2008 and the ITRF2008 (case (2) in Fig. 3).

The mean $\Delta UT1$ offsets of the satellite techniques are not given in Table 5, because these techniques are not able to determine $\Delta UT1$ in an absolute sense. To remove this rank deficiency of the GPS- and SLR-only NEQs, all $\Delta UT1$ values are fixed to the respective a priori values. The standard deviation of the mean $\Delta UT1$ offset of the combined solution is larger than the standard deviation of the VLBI solution because the combined solution contains a continuous time series of $\Delta UT1$ values. This means that since VLBI does not observe $\Delta UT1$ continuously, the offsets between the VLBI sessions are extrapolated by the satellite-technique LOD values. Due to the correlation of orbit parameters and LOD values (Bloßfeld et al. 2012a), the extrapolated $\Delta UT1$ values are systematically affected. Nevertheless, the Earth Rotation Parameters (ERP) are in a reasonable agreement with the IERS 08 C04 time series.

5.2 Epoch reference frames (ERFs)

A time series of epoch reference frames is estimated for the time span of 1994.0 to 2007.0 with a weekly resolution. In total, we computed 678 weekly reference frames of each satellite technique (GPS-only and SLR-only) and 1551 daily VLBI-only reference frames. The NEQs of these solutions were combined to 678 inter-technique weekly successive solutions. The combined NEQs contain in total 390,819 estimated parameters (Table 10).

Figure 4 shows the amount of stations per week in the epoch solution time series. The increase of GPS stations (average 149) explains almost totally the increase of the total amount of stations in the combination (average 175). The
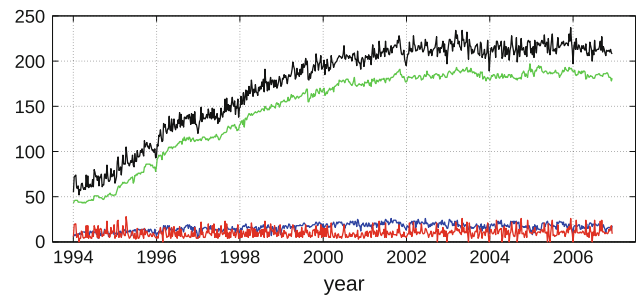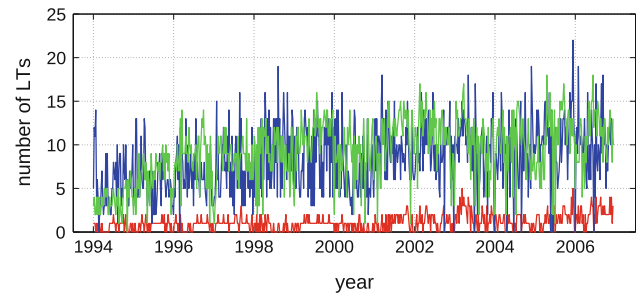
number of SLR stations (average 16) increases only slightly. The weekly amount of VLBI stations (average 10) is the sum of different stations contributing to all sessions within 1 week. The average per session is five. The number of VLBI stations is slightly increasing.

Figure 5 shows the number of introduced LTs per week between the different techniques. Compared to the increase of stations with time, the number of LTs remains nearly all the time at the same level. This is due to the fact that different thresholds are used for the LT selection (see Sect. 4.2).

5.2.1 Station coordinates

As for the MRF solutions, four different ERF solutions were computed (time series of GPS-only, SLR-only, VLBI-only and combined reference frames). For validation, the station coordinates which have been used for the datum realization are transformed epoch-wise with a 7 parameter similarity transformation to the DTRF2008. The weighted mean values of the obtained time series of transformation parameters, the respective drifts (derived from the parameter time series) and the standard deviations are summarized in Table 6.

The RMS value for the GPS-only transformation is the same as for the combined solution. The SLR-only RMS decreases in the combination due to the effect of the well-

Table 6 Weighted mean offsets of the 7 parameter similarity transformation between the computed epoch solutions and the DTRF2008 [single-technique solutions (upper part) and the technique-specific networks of the combined solution (lower part)] at epoch 2,000.0

Tech.	Par. [mm] drift [mm/a]	t_x	t_y	t_z	r_x	r_y	r_z	Sc	RMS
GPS	Parameter	0.2 ± 0.1	1.3 ± 0.0	0.0 ± 0.0	0.4 ± 0.0	-0.1 ± 0.1	0.4 ± 0.0	-0.1 ± 0.0	3.6
	Drift	-0.2 ± 0.0	0.3 ± 0.0	-0.2 ± 0.0	0.3 ± 0.0	0.0 ± 0.0	-0.1 ± 0.0	0.6 ± 0.0	
SLR	Parameter	2.6 ± 0.2	1.9 ± 0.3	1.0 ± 0.4	0.6 ± 0.2	-0.1 ± 0.2	-0.5 ± 0.2	-2.6 ± 0.2	12.7
	Drift	0.1 ± 0.1	0.0 ± 0.1	0.0 ± 0.1	0.1 ± 0.0	-0.3 ± 0.1	0.4 ± 0.1	0.1 ± 0.1	
VLBI	Parameter	0.0 ± 0.1	0.6 ± 0.1	-0.6 ± 0.1	0.4 ± 0.1	-0.7 ± 0.1	-0.3 ± 0.1	2.2 ± 0.2	8.5
	Drift	0.0 ± 0.0	0.2 ± 0.0	0.7 ± 0.0	0.3 ± 0.0	0.2 ± 0.0	0.0 ± 0.0	-0.1 ± 0.0	
Comb.	Parameter	0.4 ± 0.2	1.8 ± 0.2	0.4 ± 0.3	1.1 ± 0.1	0.2 ± 0.2	0.3 ± 0.1	0.2 ± 0.2	3.6
(GPS)	Drift	-0.2 ± 0.1	-0.3 ± 0.1	0.0 ± 0.1	0.0 ± 0.0	0.0 ± 0.0	0.0 ± 0.0	0.0 ± 0.1	
Comb.	Parameter	1.7 ± 0.2	1.2 ± 0.2	-0.6 ± 0.3	2.1 ± 0.2	-0.6 ± 0.2	-0.3 ± 0.2	-0.6 ± 0.2	10.4
(SLR)	Drift	-0.1 ± 0.1	0.1 ± 0.1	0.0 ± 0.1	0.0 ± 0.1	-0.3 ± 0.1	0.6 ± 0.1	-0.1 ± 0.1	
Comb.	Parameter	0.6 ± 0.2	4.8 ± 0.2	1.8 ± 0.2	3.8 ± 0.2	-0.4 ± 0.2	-2.7 ± 0.2	-1.9 ± 0.2	9.6
(VLBI)	Drift	-0.5 ± 0.1	-0.1 ± 0.1	0.0 ± 0.1	0.3 ± 0.0	0.2 ± 0.0	-0.1 ± 0.0	0.1 ± 0.0	

The drifts are derived from the time series of transformation parameters. The standard deviations are computed with $\sigma = \mathrm{WRMS}/\sqrt{n-1}$. Each combined epoch solution is transformed on the particular technique-specific sub-network of the DTRF2008. The Root Mean Square (RMS) of the transformation is given in the last column. The rotations and the scale are converted to displacements at the Earth's surface using the mean Earth radius $r_E = 6,378,137.0$ m

Fig. 6 *Left panel* Transformation parameter time series of the combined ERF w.r.t. the DTRF2008 in cm at the Earth's surface ($r_E = 6,378,137$ m). For the transformation, a subnet of GPS stations is used (*blue*). For comparison, the SLR-only ERF (*red*) translation and the VLBI-only ERF (*green*) scale parameters are shown. *Right panel* Amplitude spectra of the transformation parameter time series. The spectra for the VLBI-only scale parameters are not shown due to the irregular temporal resolution of the sessions
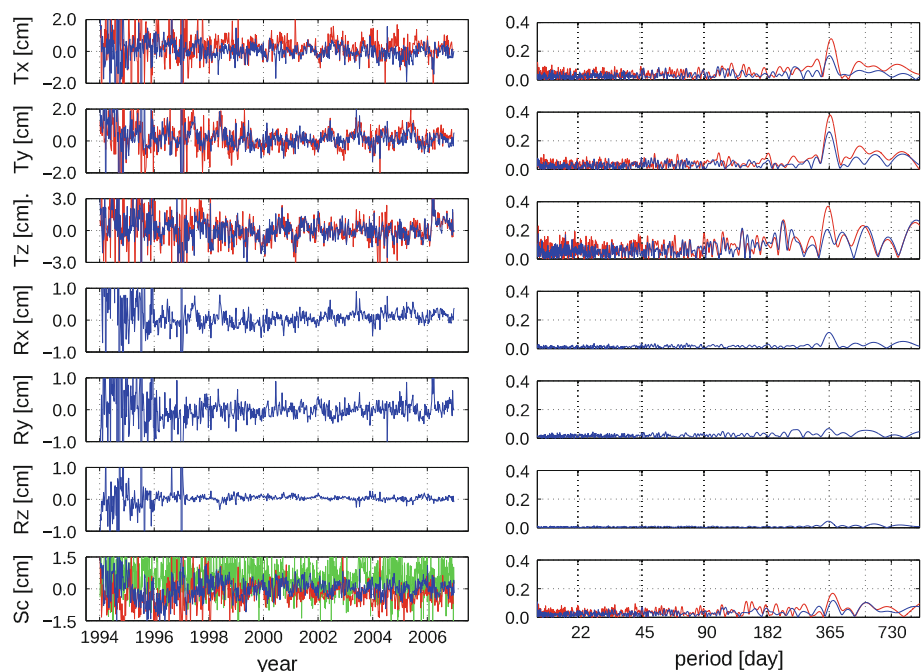
distributed GPS station network. The VLBI-only RMS increases slightly in the combination. Due to the lower number of observations, the larger impact of single outliers, the larger number of estimated parameters (Table 10) and the lower number of available LTs, the RMS values of the ERF transformations are larger than those of the MRF transformations (datum uncertainty of ERF solutions).

The left panels of Fig. 6 show the time series of transformation parameters for the GPS sub-network of the combined

ERF solutions. The right panels of Fig. 6 show the amplitude spectra of the particular time series. The three upper plots show the origin information of the SLR stations which is transferred to the GPS station via the LTs. Additionally, the translation parameters of the SLR-only ERF w.r.t. the DTRF2008 are shown. The estimated annual amplitudes and phases are summarized in Table 7. From the spectral analysis, it is clearly visible that the annual signal of the SLR-only translations is damped in the combined ERFs. This phenom-

Table 7 Annual amplitudes and phases of the transformation parameter time series shown in Fig. 6

Param.	Comb. ERF		SLR-only ERF	
	A [mm]	ϕ [°]	A [mm]	ϕ [°]
Tx	1.7 ± 0.2	179.0 ± 7.1	2.9 ± 0.4	213.2 ± 1.8
Ty	2.6 ± 0.1	290.8 ± 6.0	4.0 ± 0.0	316.9 ± 5.7
Tz	2.0 ± 0.6	233.7 ± 2.6	3.8 ± 0.7	252.3 ± 5.2
Rx	1.1 ± 0.1	287.1 ± 0.6		
Ry	0.7 ± 0.1	341.2 ± 13.4		
Rz	0.5 ± 0.0	106.3 ± 5.8		
Sc	1.1 ± 0.1	167.7 ± 11.3	1.2 ± 0.4	219.0 ± 1.8

Additionally, the amplitudes and phases for the SLR only rotations are shown

enon has two reasons. The first is the decrease of the *SLR network effect* (Collilieux et al. 2009). The *SLR network effect* is the effect of the SLR station distribution on the translation time series. Collilieux et al. (2009) compared a translation time series derived solely from SLR data (sparse network) with a time series from a combination of SLR and GPS data (dense and homogeneous network). They concluded that using a homogeneous network damps the annual amplitude at the 1 mm level and that the network effect is at the level of 1.5 mm RMS. These values are in good agreement with the amplitudes summarized in Table 7. The RMS of the SLR-only translation time series is about 1.0 mm higher than that of the combined translation time series. The second reason is the datum realization through the LTs. The GPS network gets its origin information solely from the SLR stations via the LTs. If too few LTs (less than three from different continents) are available in one week or if the global distribution of the co-located sites is sparse, the datum information would not be transferred well from one station network to the other. In extreme cases (only one or no LT available), the NEQ would not be invertible at all. In some ERFs, some outliers are still included since otherwise the number of SLR stations would be smaller than three. This means also the number of co-located sites (GPS and SLR) would be too few in the weekly solutions. On the one hand, this procedure ensures that all weekly NEQs are solvable; on the other hand, outliers in the solution affect strongly the realized datum (outliers in the transformation parameter time series) and the estimated parameters. The strong dependency of the LTs and the current SLR station distribution can be seen as a shortcoming of the ERF approach. Only if the number of LTs increases and the station network gets more homogeneous, this dependency can be reduced.

The orientation is realized by an NNR condition through a sub-network of GPS stations which is the same as for the MRF. Figure 6 (4th to 6th row) shows clearly that the remaining rotations are not zero although an NNR condition is applied. This fact is caused by the bias of the NNR condition due to the weekly $CN(t)$ variation (Sect. 2.3). Table 7 verifies the assumption that the dominating signal has also

an annual period. Since the NNR condition is applied on the GPS subnet, it can only be biased by the $CN(t)$ variation of the GPS subnet. In the time period from 1994.0 to 1996.0, the rotations are biased more than in the rest of the time series since the stations selected for the NNR condition show a rather poor global distribution. This fact leads to a bad geometry for the condition in the x- and y-rotation (subnet has small extent in north-south direction). Only the z-rotation shows smaller offsets w.r.t. DTRF2008 since the distribution has a very good extent in the east-west direction.

The scale is realized epoch-wise as an SLR and VLBI mean scale. Variations in the height component $d_h^c(t)$ of the SLR and VLBI stations, which are estimated in the ERF solutions, lead to variations in the scale parameters estimated w.r.t. an MRF, which considers only linear scale changes. Additionally, the scale is also biased due to the $CN(t)$ variation. The annual signal has nearly the same amplitude in the SLR-only and the combined ERF (about 1.1 mm).

The differences shown in Fig. 6 can be used as a validation criteria of the quality of the datum transfer from the SLR-only (origin and scale) and the VLBI-only (scale) NEQs to the GPS-only NEQs via the LTs. Thereby, the values depend strongly on the number and quality of LTs used in the combination.

In general, the mean transformation parameters of the ERFs w.r.t. the DTRF2008 are at the same order of magnitude as the transformation parameters of the MRFs. This shows the high quality of the ERF solutions. Nevertheless, outliers in all transformation parameters illustrate the datum uncertainty of the ERF solutions.

5.2.2 Earth orientation parameters

The Earth rotation parameters (x, y, UT1) of the ERFs are validated w.r.t. the IERS 08 C04 time series. The computed weighted mean offsets and the corresponding standard deviations are given in Table 8. The combined ERF solutions show an offset of -69.3 μas (-2.2 mm) for the x-pole and -2.4 μas (-0.1 mm) for the y-pole. The scatter of the MRF EOP in all solution types (Table 5) is smaller than the scat-

Table 8 Weighted mean offsets and standard deviations $\sigma = \text{WRMS}\sqrt{n-1}$ of the terrestrial pole coordinates (x, y) and (ΔUT1) of the single-technique and the combined ERFs w.r.t. the IERS 08 C04 time series

Technique	x-pole [µas]	y-pole [µas]	ΔUT1 [µs]
GPS	-77.7 ± 3.3	22.1 ± 3.0	–
SLR	-11.9 ± 11.7	-60.7 ± 11.9	–
VLBI	-71.3 ± 8.1	-9.1 ± 8.2	-3.7 ± 0.7
combination	-69.3 ± 3.6	-2.4 ± 3.4	3.8 ± 0.8

Table 9 Characteristics of the MRF and the ERF approach

	MRF	ERF
Origin	CM[a]	CM[a]
Stability	Long-term	Short-term
Parameterization	$X_s(t_0)$, $\dot{X}$	$\tilde{X}(t_i)$
Geocentric regularized position at epoch t	Mean	Instantaneous
Estimated positions	Precise	Accurate
Timeliness after earthquakes	≥ 2.5 years	Few epochs
Non-linear motions	Suppressed	Frequently sampled
Station network	Dense	Sparse
Number of LTs	High	Low
Pole coordinates	Biased	Partly biased

[a] Only if SLR data are included in the solution (SLR-only and combined MRF/ERF)

Table 10 Number n of estimated parameters in the combined MRF and ERF solutions

Frame	n (coordinates)	n (EOP)	n (all)
Comb. MRF	3,222	23,730	26,952
Comb. ERF	363,699	27,120	390,819

ter of the ERF EOP, because the stations in the MRF are only allowed to perform a linear motion. The same holds for the 08 C04 time series since it is aligned to the ITRF2008 (Fig. 3). Additionally, the piece-wise linear EOP representation allows to equalize the EOP at the week boundaries if the NEQs are accumulated (Table 10). The differences between the ERF-EOP and the MRF-EOP are studied in the spectral domain in Sect. 6.2.

6 Comparison of ERFs and MRFs

In the previous sections, the MRF and the ERF approach have been studied in detail. A summary of the characteristics is given in Table 9. Table 10 summarizes the number of parameters included in the NEQs of the different approaches. The 3,390 fewer EOP of the MRF compared to the ERF time

series can be explained by the fact that all EOP in 678 weeks are equalized at the week boundaries.

The main difference between both TRFs is that applying the combined MRF at an epoch t means getting regularized positions $X_s(t)$ in a CM frame which contain only linear motions. In contrast to this, the combined ERFs provide regularized positions $\tilde{X}(t)$ in a CM frame at every epoch t which contain linear motions as well as all non-linear motions. The differences between both positions are discussed in Sect. 6.1. The lower number of observations, the larger impact of single outliers, the larger number of estimated parameters and the lower number of available LTs in the weekly NEQs make the ERF datum more unstable compared to the MRF. Additionally, the stability condition for the MRF (linear station motions) improves the MRF long-term stability enormously. The datum realizations of the single ERFs are independent, which also leads to variations over time. The use of identical input data and common models allows to compare the MRF and ERFs and to study the non-linear station motions and their effect on other consistently estimated parameters. In Sect. 6.1, the station coordinate differences are discussed and results for the EOPs are provided in Sect. 6.2.

6.1 Station coordinates

In the following, the station coordinate estimates of the MRFs and the ERFs are compared. The differences $d(t)$ between the parameterization are the sum of the individual station motion $d^i(t)$ and the common motions to all stations $d_t^c(t)$, $d_r^c(t)$ and $d_s^c(t)$ (see Sect. 2.1). In Sect. 5, we validated the MRF and ERF w.r.t. the DTRF2008. All common station motions of the MRFs and the ERFs have been discussed there. The common station motions of the ERFs w.r.t. the MRF can be computed from an epoch-wise 7 parameter similarity transformation or from the difference of the ERF epoch datum parameter (Fig. 6) and the MRF datum parameter (Table 4) w.r.t. the DTRF2008. The remaining individual station motions in the ERFs w.r.t. the MRF are analyzed in this section.

Figure 7 shows the individual differences $d^i(t)$ between the combined ERF solutions and the combined MRF solution for the GPS stations Yarragadee in Australia between 2002.5 and 2007.5 and Irkutsk in Siberia between 1995.7 and 2007.0. The dominant signal in the time series has a seasonal period and is induced, amongst other effects, by neglected atmospheric and hydrological loading (Collilieux et al. 2009, 2012). The seasonal part can be approximated by a function composed of an annual and a semi-annual signal (sine and cosine function). This approximation is shown as a continuous line in Fig. 7. For Yarragadee, the significant annual amplitudes are between 0.5 and 1.6 mm for the horizontal station components and about 6.1 mm for the height component, respectively. For Irkutsk, the significant amplitudes in the horizontal components are 2.5 mm (north), 0.9 mm
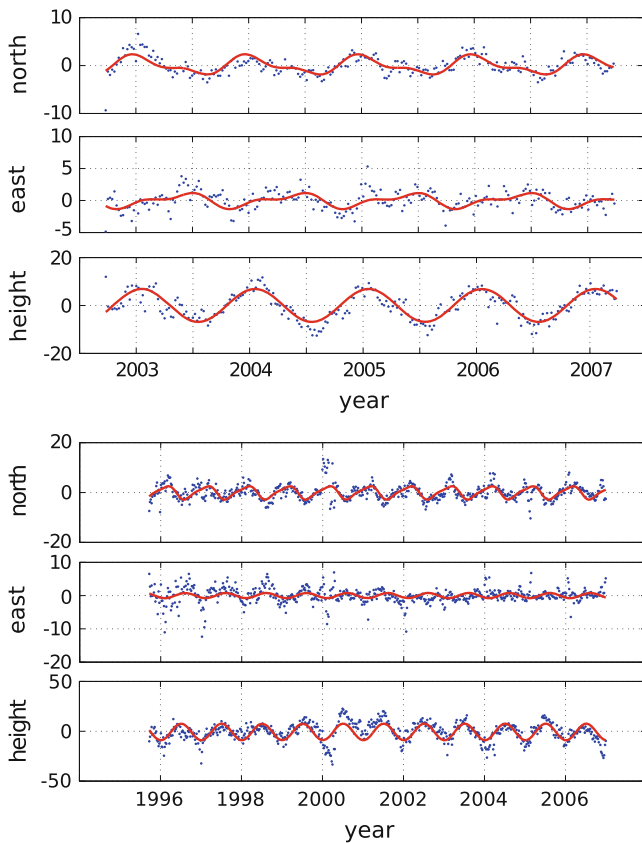
Fig. 7 Individual station position differences $d^i(t)$ [mm] (*blue dots*) between the combined ERFs and the combined MRF of the GPS stations Yarragadee (*upper plots*) and Irkutsk (*lower plots*) and a fitted annual + semi-annual signal (*red line*)

Table 11 Occurrence of annual amplitudes a [mm] in GPS residual station differences $d^i(t)$ between the ERF solution and the MRF solution

Coordinate component	$1.0 < a < 2.0$ [%]	$2.0 < a$ [%]
North	28.9	17.5
East	23.5	6.8
Height	10.9	53.4

(east) and 8.4 mm for the height. These amplitudes are at the same order of magnitude as the motions common to all stations.The results of the global analysis of the GPS stations are summarized in Table 11. More than half of the residual height differences between the combined ERFs and the combined MRF show an annual variation with an amplitude larger than 2.0 mm. But also at least 30 % of the differences in the horizontal station components show an amplitude larger than 1.0 mm. In the next section, the effect of these individual station motions on other parameters like the EOP is investigated.

6.2 Earth orientation parameters

In this section, the differences of the EOP between the MRF and the ERF solutions are discussed. At first, the analysis is done for the GPS-only solutions since these solutions are based on a very stable station network and, therefore, the EOP are estimated very accurately (smallest standard deviations). In total, two different GPS-only ERF solutions are computed:

(A) The orientation of the weekly solutions is realized by an NNR condition w.r.t. the GPS-only MRF. For the celestial pole coordinates and the ΔUT1 offsets, in each case one value is fixed to the respective a priori value at the mid-epoch of the week. This solution is the standard ERF solution.

(B) Neither the station coordinates (fixed to the MRF coordinates) nor the celestial pole coordinates or the ΔUT1 offsets (fixed to their a priori values) are estimated. This solution is an epoch-wise reconstruction of the MRF solution. Therefore, the differences of the terrestrial pole coordinates w.r.t. the MRF EOP are expected to be the smallest since the last remaining difference between the ERFs and the MRF is due to the fact that the terrestrial pole coordinates at the week boundaries are not equalized.

The EOP of the GPS-only MRF solution are subtracted from the EOP of the different GPS-only ERF solutions and the differential time series are analyzed in the frequency domain. The analysis of the amplitudes allows to quantify the effect on the terrestrial pole coordinates due to the epoch-wise estimation of the station coordinates. Figure 8 shows the amplitude spectra of the differential time series of the two GPS-only ERF solutions w.r.t. the MRF solution. As expected, solution (B) shows the smallest differences w.r.t. the MRF pole coordinates. The peaks in the x-pole at periods of 3.5 days (0.39 ± 0.04 mm) and 7 days (0.31 ± 0.04 mm) are caused by the weekly ERF interval (constraining of (UT1-UTC) at the mid-arc epoch and stacking of the EOP at the week boundaries). In the y-pole, the significant peaks are at periods of 50 days (0.20 ± 0.01 mm) and 70 days (0.18 ± 0.05 mm). These periods are multiples of the 351.15-day period, which is known as the GPS draconitic year (Ray et al. 2008; Schmid et al. 2007; Tregoning and Watson 2009). In the standard ERF solution (A), peaks at various periods are excited. The highest peaks occur at the 173- and 258-day period although their amplitudes are still below 0.6 mm. The reason why the differences of the pole coordinates have such small amplitudes in the case of GPS is twofold. On the one hand, a singularity w.r.t. the origin is created for both GPS-only TRFs (set up of translation parameters in the MRF and the ERF realization). This means, when an NNT condition is applied, the $CN(t)$ variation is absorbed by the prior intro-
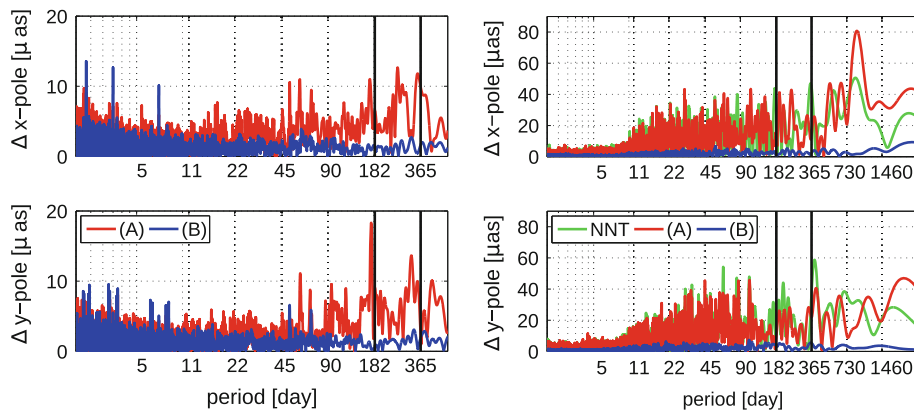
Fig. 8 Amplitude spectra of the time series of differential terrestrial pole coordinates of the GPS-only ERFs w.r.t. the GPS-only MRF (*left plots*) and of the SLR-only ERFs w.r.t. the SLR-only MRF (*right plots*). The x-pole differences are shown in the upper plots whereas the lower plots show the differences of the y-pole. *The red line* denotes solution (A), *the blue line* denotes solution (B). The SLR-only differences are filtered with a moving median filter. Additionally, in the right panels, the spectra of the SLR-only ERF solution where the datum is realized through an NNT condition is shown (*green line*)

Fig. 9 Time series of terrestrial pole coordinate differences (*black, upper plots*) between the combined ERF solutions and the combined MRF solution (both solutions are of type (A)). For computing the corresponding amplitude spectra (*lower plots*), the filtered time series (*red, upper plots*) are used
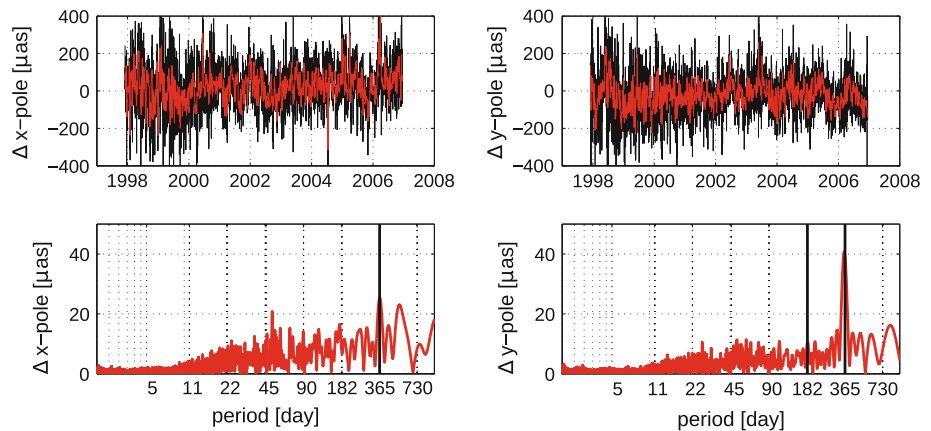
duced parameters. Therefore, the effect on the EOP is the same in both TRF realizations and no differences are caused. The only differences are due to the individually performed station motions. On the other hand, a homogeneously distributed station network for the datum realization was used (good de-correlation of translation and rotation). The results confirm that individually performed non-linear station variations partly propagate into the terrestrial pole coordinates. The differences are clearly below one millimeter but significantly estimated.

The differences for the SLR-only spectral analysis are shown in the right part of Fig. 8. For solution (B), no significant variations can be seen in the spectrum whereas for solution (A), significant variations occur. The highest amplitude of solution (A) is 2.39 ± 0.01 mm for the period 894 days. This period might be caused by superposition of other frequencies or by aliasing. Near-annual peaks with magnitudes about 1 mm can also be seen in the spectra.

Besides solution (A) and (B), a third solution type was computed for the SLR-only case. In the solution called NNT in Fig. 8, a singularity w.r.t. the origin was created and an

NNT condition was applied to realize the ERFs. Therein, the origin information is absorbed by the introduced translation parameters. Due to the fact that the EOP of the SLR-only MRF are biased because of the suppressed variation of the $CN(t)$, differences mostly in the annual frequency band with amplitudes of 1.54 ± 0.16 mm in the x-pole and 1.83 ± 0.17 mm in the y-pole are caused. One can also see that the amplitude of the 894-day signal is damped significantly. We can conclude that in the standard SLR-only ERF solution (A), the $CN(t)$ variation is partly pushed into other frequencies by the biased NNR condition.

The differential time series of the VLBI-only pole coordinates are not discussed here since the sessions mainly take place only twice a week and, therefore, the EOP time series are not continuous. In the case of the combined ERFs, only solution type (A) is compared to the combined MRF EOP. The upper part of Fig. 9 shows the terrestrial pole coordinate differences (filtered and unfiltered) of the combined solutions (ERF-MRF). The spectra of the filtered time series are shown in the lower part of Fig. 9. A dominant annual signal can be found in the y-pole differences. The amplitude is

1.23 ± 0.11 mm. In the *x*-pole differences, also an annual signal with an amplitude of 0.73 ± 0.05 mm is visible. These amplitudes are in very good agreement with the biased NNR condition (rotation parameters) in Table 7. Therein, the *x*-rotation (complementary rotation to the *y*-pole) has an annual amplitude of 1.1 ± 0.1 mm and the *y*-rotation 0.7 ± 0.1 m, respectively. This agreement shows that even the weekly GPS network does not allow a decorrelation of translations and rotations. Only if the networks will become more homogeneous in future, the ERFs can provide EOP which are more unbiased.

7 Summary

The most recent realizations of the ITRS follow the conventional secular approach. After the station position is corrected for geophysical and technique-specific effects, the regularized station motion is described by a constant position and a linear velocity. In this approach, the non-modeled motions are not considered and can bias the station position and EOP estimates, or they are absorbed by the residuals.

In this paper, we introduced an alternative approach to the conventional ITRS realization. We presented the methodology to compute epoch-wise (weekly) estimated TRFs called epoch reference frames (ERFs) from a combination of the geodetic space techniques GPS, SLR and VLBI. In this new approach, the station position is estimated weekly and thus all non-linear station motions are sampled frequently. Differences between the two parameterization, mainly caused by neglected atmospheric and hydrological loading, can be expressed as common motions to all stations and motions performed individually at a station.

We studied the characteristics of these two approaches and compared the time series of ERFs w.r.t. the secular approach. Thereby, we investigated the stability of the datum realization and we analyzed the differences in the station positions and terrestrial pole coordinates. We found that individual non-linear station motions bias into other parameters of the secular approach. The common motions cause systematic differences in the datum realization of both TRFs. The orientation of the secular TRF is affected by an offset and a drift, whereas the ERF orientation is affected by weekly offsets. Since we deal with an imperfect globally distributed station network, the geocentric NNR and NNS conditions are biased by non-linear variations in the barycenter of the ERFs. In the secular TRFs, this variation is suppressed and partly forced into the pole coordinates (complementary parameters to network orientation). It is a matter of fact that the more sparse the global station distribution, the higher are the correlations between the datum parameters.

Even if we use a subset of the IGS station network for the NNR condition, we found annual signals with 23.6 μas to 39.8 μas amplitude in the pole coordinate differences of the combined solutions. When the pole coordinates of the SLR-only TRFs are compared, even larger amplitudes (77.3 μas) can be found. This effect can only be reduced (but never eliminated) if it would be possible to choose an ideal station network for the datum realization. Then, the ERFs could provide nearly unbiased EOP and quasi-instantaneous station positions in one common adjustment.

Another critical issue for the TRF computation is the local ties. In the conventional approach, all existing co-location sites can be used for the combination. For the ERF computation, only the co-location sites can be used which observe during the particular week. Therefore, the number and global distribution of available local ties is reduced. To minimize the datum instability and the aliasing effects in the datum realization, global well-distributed stations with an adequate number of co-location sites are necessary. These requirements are part of the aim of the Global Geodetic Observing System (GGOS).

Since the availability of improved networks will take some time, we have to think about other ways to stabilize the datum and minimize the aliasing effects. One possibility could be to extend the weekly time interval to 14 or 28 days. With a longer time interval, the network geometry and the number of LTs might be improved. One can also think about including DORIS in the combination since this technique has a homogeneous station distribution with numerous co-locations to the other techniques.

If a stable datum and unbiased EOP can be achieved, the ERFs will be valuable for (i) the supporting of secular ITRF realizations to ensure accurate station positions with high timeliness, (ii) monitoring non-linear station motions (geophysical and anthropogenic phenomena), (iii) the determination of EOP since the strengths of all techniques are used and the EOP are unbiased, (iv) geophysicists who need coordinate time series in a *CM* frame to interpret geophysical phenomena and validate their models.

References

Altamimi Z, Collilieux X, Métivier L (2011) ITRF2008: an improved solution of the international terrestrial reference frame. J Geodesy 85(8):457–473. doi:10.1007/s00190-011-0444-4

Altamimi Z, Sillard P, Boucher C (2002),ITRF2000: a new release of the International Terrestrial ReferenceFrame for earth science applications. J Geophys Res 107(B10).doi:10.1029/2001JB000561

Angermann D, Drewes H, Krügel M, Meisel B (2007) Advances in terrestrial reference frame computations. In: Tregoning P, Rizos C, Sanso F (eds) Dynamic planet. International association of geodesy symposia, vol 130. Springer, Berlin, pp 595–602. doi:10.1007/978-3-540-49350-186

Angermann D, Drewes H, Krügel M, Meisel B, Gerstl M, Kelm R, Müller H, Seemüller W, Tesmer V (2004) ITRS Combination Center at DGFI: a terrestrial reference frame realization 2003. Reihe B, Verlag der Bayerischen Akademie der Wissenschaften

Bawden GW, Thatcher W, Stein RS, Hudnut KW, Peltzer G (2001) Tectonic contraction across Los Angeles after removal of groundwater pumping effects. Lett Nat 412:812–815. doi:10.1038/35090558

Bevis M, Alsdorf D, Kendrick E, Fortes LP, Forsberg B, Smalley R, Jr, Becker J (2005) Seasonal fluctuations in the mass of the Amazon River system and Earth's elastic response. Geophys Res Lett 32(L16308). doi:10.1029/2005GL023491

Blewitt G (2003) Self-consistency in reference frames, geocenter definition, and surface loading of the solid. Earth, J Geophys Res 108(B2). doi:10.1029/2002JB008082

Blewitt G, Lavallée D (2002) Effect of annual signals on geodetic velocity. J Geophys Res 107(B7). doi:10.1029/2001JB000570

Bloßfeld M, Müller H, Angermann D (2012a) Adjustment of EOP and gravity field parameters from SLR observations. In: Proceedings of the 17th international workshop on laser ranging. Verlag des Bundesamtes für Kartographie und Geodäsie, Frankfurt am Main, Mitteilungen des Bundesamtes für Kartographie und Geodäsie

Bloßfeld M, Müller H, Seitz M, Angermann D (2012b) Benefits of SLR in epoch reference frames. In: Proceedings of the 17th international workshop on laser ranging. Verlag des Bundesamtes für Kartographie und Geodäsie, Frankfurt am Main, Mitteilungen des Bundesamtes für Kartographie und Geodäsie

Böckmann S, Artz T, Nothnagel A, Tesmer V (2007) Comparison and combination of consistent VLBI solutions. In: Proceedings of the 18th European VLBI for geodesy and astronomy working meeting. Wien, Geowissenschaftliche Mitteilungen

Bürgmann R, Dresen G (2008) Rheology of the lower crust and upper mantle: evidence from rock, mechanics, geodesy, and field observations. Annu Rev Earth Planet Sci 36:531–567. doi:10.1146/annurev.earth.36.031207.124326

Collilieux X, van Dam T, Ray J, Coulot D, Métivier L, Altamimi Z (2012) Strategies to mitigate aliasing of loading signals while estimating GPS frame parameters. J Geodesy 86(1):1–14. doi:10.1007/s00190-011-0487-6

Collilieux X, Altamimi Z, Ray J, van Dam T, Wu X (2009), Effect of the satellite laser ranging network distribution on geocenter motion estimates. J Geophys Res 114(B4). doi:10.1029/2008.JB005727

Davis JL, Wernicke BP, Tamisiea ME (2012), On seasonal signals in geodetic time series. J Geophys Res 117(B1). doi:10.1029/2011JB008690

Dong D, Yunck T, Heflin M (2003), Origin of the international terrestrial reference frame. J Geophys Res 108(B4). doi:10.1029/2002JB002035

Förste C, Schmidt R, Stubenvoll R, Flechtner F, Meyer U, König R, Neumayer H, Biancale R, Lemoine JM, Bruinsma S, Barthelmes F, Esselborn S (2008) The GeoForschungsZentrum Potsdam/Groupe de Recherche de Gèodésie Spatiale satellite-only and combined gravity field models: EIGEN-GL04S1 and EIGEN-GL04C. J Geodesy 82(6):331–346. doi:10.1007/s00190-007-0183-8

Freymueller JT (2010) Active tectonics of plate boundary zones and the continuity of plate boundary deformation from Asia to North America. Curr Sci 99(12):1719–1732

Gerstl M (1997) Parameterschätzung in DOGS-OC, 2nd edn. DGFI Int. Bericht Nr. MG/01/1996/DGFI

Gerstl M, Kelm R, Müller H, Ehrensperger W (2001) DOGS-CS Kombination und Lösung gro-ßer Gleichungssysteme. DGFI Int. Bericht Nr. MG/01/1995/DGFI

Koch KR (1997) Parameterschätzung und Hypothesentests in linearen Modellen, 3rd edn. Dummler, Bonn. ISBN 3427789233

Kreemer C, Lavallée DA, Blewitt G, Holt WE (2006) On the stability of a geodetic no-net-rotation frame and its implication for the International Terrestrial Reference Frame. Geophys Res Lett 133(17): doi:10.1029/2006GL027058

Listing JB (1873) Über unsere jetzige Kenntnis der Gestalt und Größe der Erde. Nachr. d. Kgl. Gesellsch. d. Wiss. und der Georg-August-Univ, Göttingen, pp 33–98

Meisel B, Angermann D, Krügel M, Drewes H, Gerstl M, Kelm R, Müller H, Seemüller W, Tesmer V (2005) Refined approaches for terrestrial reference frame computations. Adv Space Res 36(3):350–357. doi:10.1016/j.asr.2005.04.057

Nothnagel A (2009) Conventions on thermal expansion modelling of radio telescopes for geodetic and astrometric VLBI. J Geodesy 83(8):787–792. doi:10.1007/s00190-008-0284-z

Petit G, Luzum B (2010) IERS Conventions (2010). IERS Technical Note 36, Verlag des Bundesamtes für Kartographie und Geodäsie, ISBN 978-3-89888-989-6

Petrov L, Boy JP (2004), Study of the atmospheric pressure loading signal in very long baseline interferometry observations. J Geophys Res 109(B3). doi:10.1029/2003JB002500

Ray J, Altamimi Z, Collilieux X, van Dam T (2008) Anomalous harmonics in the spectra of GPS position estimates. GPS Solut 12(1):55–64. doi:10.1007/s10291-007-0067-7

Rothacher M, Angermann D, Artz T, Bosch W, Drewes H, Böckmann S, Gerstl M, Kelm R, König D, König R, Meisel B, Müller H, Nothnagel A, Panafidina N, Richter B, Rudenko S, Schwegmann W, Seitz M, Steigenberger P, Tesmer V, Thaller D (2011) GGOS-D: homogeneous reprocessing and rigorous combination of space geodetic observations. J Geodesy 85(10):679–705. doi:10.1007/s00190-011-0475-x

Sarti P, Abbondanza C, Petrov L, Negusini M (2011) Height bias and scale effect induced by antenna gravitational deformation in geodetic VLBI data analysis. J Geodesy 85(1):1–8. doi:10.1007/s00190-010-0410-6

Schmid R, Steigenberger P, Gendt G, Ge M, Rothacher M (2007) Generation of a consistent absolute phase center correction model for GPS receiver and satellite antennas. J Geodesy 81(12):781–798. doi:10.1007/s00190-007-0148-y

Schön S, Kutterer HJ (2007) A comparative analysis of uncertainty modelling in GPS data analysis. In: Tregoning P, Rizos C, Sideris MG (eds) Dynamic planet, international association of geodesy symposia, vol 130, Springer, Berlin, pp 137–142. doi:10.1007/978-3-540-49350-1_22

Seitz M (2009) Kombination geodätischer Raumbeobachtungsverfahren zur Realisierung eines terrestrischen Referenzsystems. Reihe C, Verlag der Bayerischen Akademie der Wissenschaften

Seitz M, Angermann D, Bloßfeld M, Drewes H, Gerstl M (2012) The DGFI realization of ITRS: DTRF2008. J Geodesy 86(12):1097–1123. doi:10.1007/s00190-012-0567-2

Suito H, Freymueller JT (2009), A viscoelastic and afterslip postseismic deformation model for the 1964 Alaska earthquake. J Geophys Res 114(B11). doi:10.1029/2008JB005954

Thaller D (2008) Inter-technique combination based on homogeneous equation systems including station coordinates, Earth orientation and troposphere parameters. Scientific Technical Report STR 08/15, Deutsches GeoForschungsZentrum (GFZ), doi:10.2312/GFZ.b103-08153

Torge W (2001) Geodesy. 3rd edn. deGruyter, Berlin. ISBN 3-11-017072-8

Tregoning P, van Dam T (2005), Effects of atmospheric pressure loading and seven-parameter transformations on estimates of geocenter

motion and station heights from space geodetic observations. J Geophys Res 110(B3). doi:10.1029/2004JB003334

Tregoning P, Watson C (2009), Atmospheric effects and spurious signals in GPS analyses. J Geophys Res 114(B9). doi:10.1029/2009JB006344

van Dam TM, Blewitt G, Heflin B (1994) Atmospheric pressure loading effects on Global Positioning System coordinate determinations. J Geophys Res 99(12):23939–23950. doi:10.1029/94JB02122

van Dam TM, Collilieux X, Wuite J, Altamimi Z, Ray J (2012) Nontidal ocean loading: amplitudes and potential effects in GPS height time series. J Geodesy 86(11):1043–1057. doi:10.1007/s00190-012-0564-5

Wu X, Ray J, van Dam T (2012) Geocenter motion and its geodetic and geophysical implications. J Geodyn 58:44–61. doi:10.1016/j.jog.2012.01.007